

Measurements of $H \rightarrow W^+W^-$ in the Fully Leptonic Decay Mode at the FCC-ee

Kael Kemp ,* Aman Desai ,[†] and Paul Jackson ,[‡]

Department of Physics, Adelaide University, North Terrace, Adelaide, SA 5005, Australia

(Dated: January 30, 2026)

The expected precision on measuring the $\sigma(e^+e^- \rightarrow ZH) \times Br(H \rightarrow W^+W^-)$ in the fully leptonic decay mode at the Future Circular Collider (FCC) is presented. We consider two FCC-ee scenarios: $\sqrt{s} = 240$ GeV centre-of-mass energy with a luminosity of 10.8 ab^{-1} and $\sqrt{s} = 365$ GeV centre-of-mass energy with a luminosity of 3.12 ab^{-1} . Our results indicate that a relative uncertainty of 2.9% and 6.8% can be achieved on measurements of $\sigma(e^+e^- \rightarrow ZH) \times Br(H \rightarrow W^+W^-)$ in the fully leptonic decay mode at $\sqrt{s} = 240$ GeV and $\sqrt{s} = 365$ GeV, respectively.

I. INTRODUCTION

The discovery of Higgs boson by the ATLAS and CMS collaborations at the Large Hadron Collider (LHC) completed the Standard Model [1–4]. The Higgs boson is the key to understanding the electroweak symmetry breaking mechanism, which gives masses to the Z and W^\pm gauge bosons. The Higgs boson couplings to the gauge bosons and third generation fermions have been studied at the LHC, showing consistency with the Standard Model predictions [5, 6]. Studying the properties of the Higgs boson with precision is one of the major goals of the Future Circular Collider (FCC), a proposed collider facility at CERN [7–9]. The FCC-ee will collide electrons and positrons at centre-of-mass energies ranging from the Z -pole (91 GeV) up to the top-quark pair production threshold (365 GeV). Collisions at $\sqrt{s} = 240$ GeV will be important for performing Higgs measurements, as the Higgs production cross-section in the Higgs-strahlung (ZH) channel is maximal at this energy, $\sigma(e^+e^- \rightarrow ZH) \approx 200 \text{ fb}$ [7]. With a predicted integrated luminosity of 10.8 ab^{-1} at this collision energy, FCC-ee would produce approximately 2.2×10^6 Higgs bosons. Additionally, Higgs measurements will also be possible at $\sqrt{s} = 365$ GeV with a proposed integrated luminosity of 3.1 ab^{-1} , where the cross-section in the ZH channel is $\approx 125 \text{ fb}$ [7].

The branching fraction for the Higgs decay to WW^1 is $\sim 21\%$, which makes it the second most common decay channel after the $b\bar{b}$ channel [10]. The Higgs coupling to W bosons can be measured by analysing the $H \rightarrow WW$ decay channel. In this work, the decays of the Z and W bosons to leptons are considered, which gives rise to a final state consisting of four leptons and missing energy. The fully leptonic decay mode have relatively low branching fractions when compared to modes involving jets. The absence of pileup at FCC-ee and the final state consisting of no jets initiated by hadronisation of quarks leads to a higher precision measurement of $ZH[WW]$.

In this analysis, we study $Z(\ell\ell)H[WW(\ell\ell\nu\nu)]$, with ℓ being either an electron or a muon, at centre-of-mass energies $\sqrt{s} = 240, 365$ GeV. A survey of different decay modes - or - combination of electrons and muons is carried out. In particular, we consider the channels consisting of two electrons and two muons, three electrons (one electron) and one muon (three muons), four electrons, and four muons. We assess the impact of different leptonic decays on the relative uncertainty of the measurements.

This paper is organised as follows: in Section II, we discuss the Monte Carlo samples used in this analysis. The preselection criteria used to prepare samples for the six different channels are discussed in Section III. In Section IV, we present the analysis strategy, that includes a cut-flow and also a Machine Learning based ap-

* kael.kemp@adelaide.edu.au

[†] aman.desai@adelaide.edu.au

[‡] p.jackson@adelaide.edu.au

¹ Throughout this paper, we assume charge conjugation.

proach. Finally, the signal strength when measuring the $\sigma(e^+e^- \rightarrow ZH) \times Br(H \rightarrow WW)$ is determined in Section V.

II. EVENT SIMULATION

The Monte Carlo samples used in this study were produced centrally by the FCC Collaboration and are tagged as the WINTER2023 campaign [11]. The signal and the background samples used in this analysis that included a Higgs boson were generated using WHIZARD [12] followed by PYTHIA6 [13] for hadronisation and parton shower. The decays of $H \rightarrow WW$ and $H \rightarrow ZZ$ are inclusive. The background samples, ZZ , WW , and $t\bar{t}$, were generated using PYTHIA8 [14] and also consider inclusive decays of the gauge bosons.

The generated events are then passed through the DELPHES fast simulation package [15] to simulate the parametric response of the proposed IDEA detector [16]. The implementation is such that electron and muon tracks with $p_T > 100$ MeV and $|\eta| < 2.56$ are assumed to be reconstructed with 100% efficiency. Smearing is applied, taking into account the detector resolution and also scattering of particles by detector material. Identification efficiency for electrons and muons is set to 99% for $E > 2$ GeV and $|\eta| < 3$. The imbalance in energy is identified as E^{miss} .

This event generation chain is implemented in the KEY4HEP software [17]. The configuration files used in the production can be found in Ref. [18].

In this study, the right-handed coordinate system is used. The interaction point is the centre of the IDEA detector and is used as the origin of this coordinate system. The x-axis points towards the centre of the FCC-ee and the y-axis points upwards. The z-axis points in the beam direction, and the azimuthal angle is measured from the x-axis.

Table I gives a list of all the samples used in this study for $\sqrt{s} = 240$ GeV, along with the cross-sections, and the number of events generated. The corresponding table for $\sqrt{s} = 365$ GeV is given in Table II. At this energy,

contribution from Vector Boson Fusion is significant in processes such as e^+e^-H and $\nu\bar{\nu}H$. The samples labelled as $ZH[WW]$ consider the decay of the Z boson to either a pair of electrons or a pair of muons.

III. EVENT PRESELECTION

We carry out these analyses using the FCCANALYSES software framework [19]. The analysis for $\sqrt{s} = 240$ GeV and $\sqrt{s} = 365$ GeV is carried over six orthogonal final states which are listed in Table III.

As a general strategy, events consisting of at least four leptons satisfying the condition $|\vec{p}_\ell| > 5$ GeV are pre-selected. As our final state consists of neutrinos, which escape the detector without detection, we also require $E_{\text{miss}} > 5$ GeV.

Each final state considered in this study is processed through a set of channel specific preselection criteria. These criteria are in place to ensure the different sub-analyses remain orthogonal – which is useful when carrying out statistical combination of different channels. We achieve this in the following way: in the **ZeeH_{mumu}** and **Z_{mumu}H_{ee}** channels we require exactly two electrons and two muons, $N_e = 2$ and $N_\mu = 2$ with an additional requirement of net charge of the muons and electrons being zero: $\sum_e N_Q = 0$ and $\sum_\mu N_Q = 0$. For the **ZeeH_{emu}** (**Z_{mumu}H_{emu}**) channels we require $N_e = 3$, $N_\mu = 1$, ($N_\mu = 3$ and $N_e = 1$). For these channels, we require that the net charge of all leptons to be equal to zero. For the **ZeeH_{ee}** (**Z_{mumu}H_{mumu}**), we require $N_e = 4$ and $N_\mu = 0$ ($N_\mu = 4$ and $N_e = 0$). Again, the net charge of all leptons is required to be equal to zero.

The final state leptons are then used to reconstruct the Z boson, considering the Z boson having a mass of 91 GeV. In **ZeeH_{mumu}** (**Z_{mumu}H_{ee}**), which consists of exactly two electrons (muons) coming from the decay of the Z boson, the Z boson is reconstructed by summing the four-momenta of the same flavour but opposite sign leptons. In the **ZeeH_{emu}** and **Z_{mumu}H_{emu}** channels, an additional combinatoric step is performed to find the combination of leptons with net-zero charge, the same flavour and

Table I: The list of processes considered in this analysis, their production cross-section at $\sqrt{s} = 240$ GeV and number of events.

Label	Process	Cross section [fb]	N_{events}
Signal			
$ZH[WW]$	$e^+e^- \rightarrow Z(\mu^+\mu^-)H(WW^*)$	1.46	400,000
	$e^+e^- \rightarrow Z(e^+e^-)H(WW^*)$	1.54	400,000
Background			
WW	$e^+e^- \rightarrow W^+W^-$	1.64×10^4	3.73×10^8
ZZ	$e^+e^- \rightarrow ZZ$	1.36×10^3	5.62×10^8
	$e^+e^- \rightarrow Z(\tau^+\tau^-)H(WW^*)$	1.45	400,000
	$e^+e^- \rightarrow Z(\mu^+\mu^-)H(ZZ^*)$	0.18	400,000
	$e^+e^- \rightarrow Z(e^+e^-)H(ZZ^*)$	0.19	400,000
ZH	$e^+e^- \rightarrow Z(\nu\bar{\nu})H(ZZ^*)$	1.22	1,200,000
	$e^+e^- \rightarrow Z(e^+e^-)H(\tau^+\tau^-)$	4.49	400,000
	$e^+e^- \rightarrow Z(\mu^+\mu^-)H(\tau^+\tau^-)$	0.42	400,000
	$e^+e^- \rightarrow Z(\tau^+\tau^-)H(\mu^+\mu^-)$	1.47×10^{-3}	400,000
	$e^+e^- \rightarrow Z(\tau^+\tau^-)H(ZZ^*)$	0.18	330,996
	$e^+e^- \rightarrow Z(\tau^+\tau^-)H(\tau^+\tau^-)$	0.42	400,000

their invariant mass closest to the Z boson mass. The **ZeeHee** and **ZmumuHmumu** present a combinatorics challenge, wherein the best resonance is to be found from a set of combinations of electrons or muons, with opposite sign, and choosing the pair which gives the least difference in the invariant mass of lepton pair and the Z boson mass.

The pair of leptons that is not used to reconstruct the Z boson resonance is then assumed to be coming from the $H \rightarrow WW$ decays. We label this pair separately, as these variables can enable us to discriminate against the background arising from ZZ .

Furthermore, we also reconstruct the recoil mass as the Z boson recoils against the Higgs boson. This variable is computed based on energy-momentum conservation and also information about the initial state, which is well known at the e^+e^- collider. This quantity in the $Z(\ell\ell)H$ case is given as:

$$m_{\text{recoil}}^2 = s + m_Z^2 - 2E_Z\sqrt{s} \quad (1)$$

where the energy and the invariant mass of the Z boson are computed by combining the lepton pair as discussed earlier. The variable is such that it peaks near the invariant mass of the recoiling object, which in the case of the signal, is the Higgs boson mass (125 GeV). As the background ZZ and WW do not contain a Higgs boson, they are not likely to peak near the Higgs mass, allowing us to use this quantity as a handle to discriminate signal from the background.

The resulting yield after applying these preselection conditions are summarised for $\sqrt{s} = 240$ GeV and $\sqrt{s} = 365$ GeV in Table IV and Table V, respectively. The ZZ process remains a dominant source of background across all channels.

The distributions of the variables studied in this anal-

Table II: The list of processes considered in this analysis, their production cross-section at $\sqrt{s} = 365$ GeV and number of events.

Label	Process	Cross section [fb]	N_{events}
Signal			
ZH[WW]	$e^+e^- \rightarrow Z(\mu^+\mu^-)H(WW^*)$	0.90	1,100,000
	$e^+e^- \rightarrow e^+e^-H(WW^*)$	1.59	1,100,000
Background			
WW	$e^+e^- \rightarrow W^+W^-$	1.07×10^4	1.01×10^8
ZZ	$e^+e^- \rightarrow ZZ$	6.43×10^2	6.14×10^7
$t\bar{t}$	$e^+e^- \rightarrow t\bar{t}$	8.00×10^2	2,700,000
ZH	$e^+e^- \rightarrow Z(\tau^+\tau^-)H(WW^*)$	0.90	1,100,000
	$e^+e^- \rightarrow Z(\mu^+\mu^-)H(ZZ^*)$	0.11	800,000
	$e^+e^- \rightarrow e^+e^-H(ZZ^*)$	0.20	1,200,000
	$e^+e^- \rightarrow \nu\bar{\nu}H(ZZ^*)$	1.42	1,200,000
	$e^+e^- \rightarrow e^+e^-H(\tau^+\tau^-)$	0.46	1,200,000
	$e^+e^- \rightarrow Z(\mu^+\mu^-)H(\tau^+\tau^-)$	0.26	900,000
	$e^+e^- \rightarrow Z(\tau^+\tau^-)H(\mu^+\mu^-)$	9.08×10^{-4}	1,200,000
	$e^+e^- \rightarrow Z(\tau^+\tau^-)H(ZZ^*)$	1.10	1,200,000
	$e^+e^- \rightarrow Z(\tau^+\tau^-)H(\tau^+\tau^-)$	0.26	1,100,000

Table III: The leptonic decay modes considered in this study and their corresponding labels.

Final State	Label
$Z(\mu\mu), H[WW(ee\nu\nu)]$	ZmumuHee
$Z(\mu\mu), H[WW(e\mu\nu\nu)]$	ZmumuHemu
$Z(\mu\mu), H[WW(\mu\mu\nu\nu)]$	ZmumuHmumu
$Z(ee), H[WW(ee\nu\nu)]$	ZeeHee
$Z(ee), H[WW(e\mu\nu\nu)]$	ZeeHemu
$Z(ee), H[WW(\mu\mu\nu\nu)]$	ZeeHmumu

ysis, after applying preselection criteria, are given in Figure 1 ($\sqrt{s} = 240$ GeV) and Figure 3 ($\sqrt{s} = 365$ GeV).

IV. ANALYSIS STRATEGY

For each final state the analysis is performed separately in two stages. The first stage involves determining a set of selection criterion based on the distributions of the observables, motivated by improving significance at each step by rejecting the background events. Here, the significance is defined as $S/\sqrt{S+B}$. In the second stage, Multivariate Analysis (MVA) methods are applied to the signal and background events to find a discriminator that could improve the significance of the observation.

In Table IV, we present a set of selection criteria and the corresponding yields for the signal and background processes at $\sqrt{s} = 240$ GeV. The preselection criteria defined earlier lead to an initial significance of $\approx 1.8\sigma$ in the ZmumuHee and $\approx 1.9\sigma$ in the ZeeHmumu channels. In the channels consisting of four electrons or four muons, the preselection significance is $\approx 2.5\sigma$ and 2.6σ , respectively.

Due to the absence of major backgrounds consisting of three muons and one electron (one muon and three electrons), the **ZmumuHemu** (**ZeeHemu**) show a significance of about ≈ 5.4 (4.9σ).

We begin the selection criteria by requiring at least one pair of leptons with invariant mass consistent with the mass of the Z boson. In all channels, this selection criteria reduces the background from the WW process, as expected, due to the absence of a Z boson. Moreover, an upper selection criteria on the lepton momenta is useful to remove background events from the ZZ and WW processes.

For the signal sample, the recoil mass is expected to be close to the Higgs boson mass. This additional observable can be used to reject events not consistent with the presence of the Higgs boson as an intermediate quantum state. Furthermore, we select events satisfying $|\eta_{\text{miss}}| < 2.0$ motivated by the presence of neutrinos in final state in this region.

The results from the selection based analysis show that we achieve 8.1σ and 8.4σ in **ZmumuHee** and **ZeeHmumu** channels, respectively. For these channels, the background is mainly dominated by the $e^+e^- \rightarrow ZH(\rightarrow ZZ)$ process where two Z bosons decay into leptons and one of the Z bosons decays to a pair of neutral leptons. In the four muons and four electrons channels, **ZmumuHmumu** and **ZeeHee** give a significance of 8.2σ and 7.4σ , respectively. Here, the background is dominated by $e^+e^- \rightarrow ZZ$ which yields exactly the same visible final state, followed by contributions from ZH processes. Across all channels, the highest significance, of 12.1σ and 12.8σ is noted in the **ZeeHemu** and **ZmumuHemu** channels, respectively.

We also developed a Machine Learning based approach to improve sensitivity when discriminating the signal from the background. We used a Boosted Decision Tree (BDT) from XGBoost package [20] for a signal versus background classification task. A set of both, low-level features, including the four-momenta of the leptons, missing momenta and the associated pseudorapidity, visible energy and transverse visible momenta, and high level features such as the invariant mass of the dilepton pairs, angular distance between leptons, mass and energy of Z boson and

the recoil mass are used. We also evaluated the fraction of missing energy over the total energy. Angular variables based on the ΔR distance between pairs of all possible leptons is evaluated using the following equation:

$$\Delta R(\ell_1, \ell_2) = \sqrt{\Delta\phi^2(\ell_1, \ell_2) + \Delta\eta^2(\ell_1, \ell_2)} \quad (2)$$

We used 44 features to train the BDT. The parameters defining the BDT model are summarised in Table VI. The set of parameters are chosen so as not to overfit or underfit the training dataset. The binary logistic function is used for binary classification. The maximum depth of each tree is set to five to prevent overfitting. The number of estimators is set to 1000, while early stopping rounds are set to 50. Several parameters, such as regularisation, were employed to further reduce overfitting. The preselected events are used to train and test the model. These events are split into two sets: training and testing phase, with a ratio of 3:1. We train the model for each given channel separately, and the results obtained are saved using the ROOT TMVA feature [21] in order to assess the impact on the entire set of event samples. The outcome of the MVA on the preselected events is presented in Figure 2 for all six channels at 240 GeV.

Across all channels, we selected events satisfying MVA score greater than 0.6. This leads to an improvement in significance in all channels. The **ZmumuHee** and **ZeeHmumu** channel sees an increase in significance by 58% and 51%, respectively. In the **ZmumuHmumu** a rise in significance by 53% is noted while the **ZeeHee** channels has an improvement of about 66% in signal versus background discrimination. In the **ZmumuHemu** and **ZeeHemu** channels, the significance shows an improvement by about 48% and 53%, respectively. This approach show an increase in significance to up to $\sim 12.3\sigma$ to 19σ in **ZeeHee** and **ZmumuHemu** channels, respectively.

A similar approach is followed for analysing $\sqrt{s} = 365$ GeV. In Table V, a set of selection criterion along with the expected yields are presented. The preselection criteria introduced in the previous section lead to the following significance: 0.6σ in **ZmumuHee**; 0.9σ in **ZeeHmumu**

Table IV: Event yields and significance for all channels at $\sqrt{s} = 240$ GeV after applying selection conditions.

(a) ZmumuHee							(b) ZeeHmumu						
Selection	<i>S</i>	<i>B_{ZZ}</i>	<i>B_{WW}</i>	<i>B_{ZH}</i>	<i>B_{tot}</i>	<i>Z</i>	Selection	<i>S</i>	<i>B_{ZZ}</i>	<i>B_{WW}</i>	<i>B_{ZH}</i>	<i>B_{tot}</i>	<i>Z</i>
Preselection	240	15139	1947	356	17442	1.8	Preselection	250	15139	1947	356	17442	1.9
$80 < m_Z < 100$ GeV	216	6821	171	161	7152	2.5	$80 < m_Z < 100$ GeV	208	6325	68	149	6542	2.5
$p_\ell < 80$ GeV	216	3794	134	160	4088	3.3	$p_\ell < 80$ GeV	208	3536	48	149	3733	3.3
$110 < m_{\text{recoil}} < 150$ GeV	215	2074	104	158	2336	4.3	$110 < m_{\text{recoil}} < 150$ GeV	207	2000	38	146	2184	4.2
$ \eta_{\text{miss}} < 2$	207	211	96	144	451	8.1	$ \eta_{\text{miss}} < 2$	200	195	36	133	363	8.4
MVA > 0.6	168	2	2	1	5	12.8	MVA > 0.6	165	0	2	1	4	12.7
Cumulative Efficiency (%)	70	0	0	0	0	—	Cumulative Efficiency (%)	66	0	0	0	0	—

(c) ZmumuHmumu							(d) ZeeHee						
Selection	<i>S</i>	<i>B_{ZZ}</i>	<i>B_{WW}</i>	<i>B_{ZH}</i>	<i>B_{tot}</i>	<i>Z</i>	Selection	<i>S</i>	<i>B_{ZZ}</i>	<i>B_{WW}</i>	<i>B_{ZH}</i>	<i>B_{tot}</i>	<i>Z</i>
Preselection	235	7358	407	162	7926	2.6	Preselection	253	7566	1904	177	9647	2.5
$80 < m_Z < 100$ GeV	217	5635	91	138	5864	2.8	$80 < m_Z < 100$ GeV	218	5432	314	143	5889	2.8
$p_\ell < 80$ GeV	216	2989	53	137	3179	3.7	$p_\ell < 80$ GeV	218	2997	198	142	3337	3.7
$110 < m_{\text{recoil}} < 150$ GeV	213	1551	45	135	1731	4.8	$110 < m_{\text{recoil}} < 150$ GeV	214	1610	164	140	1914	4.6
$ \eta_{\text{miss}} < 2$	206	267	43	124	435	8.1	$ \eta_{\text{miss}} < 2$	206	291	156	129	576	7.4
MVA > 0.6	161	4	3	1	8	12.4	MVA > 0.6	160	5	3	2	10	12.3
Cumulative Efficiency (%)	69	0	1	1	0	—	Cumulative Efficiency (%)	63	0	0	1	0	—

(e) ZmumuHemu							(f) ZeeHemu						
Selection	<i>S</i>	<i>B_{ZZ}</i>	<i>B_{WW}</i>	<i>B_{ZH}</i>	<i>B_{tot}</i>	<i>Z</i>	Selection	<i>S</i>	<i>B_{ZZ}</i>	<i>B_{WW}</i>	<i>B_{ZH}</i>	<i>B_{tot}</i>	<i>Z</i>
Preselection	478	6238	853	241	7332	5.4	Preselection	498	6359	3346	254	9958	4.9
$80 < m_Z < 100$ GeV	435	3537	41	189	3767	6.7	$80 < m_Z < 100$ GeV	419	3409	111	183	3703	6.5
$p_\ell < 80$ GeV	434	1903	20	188	2111	8.6	$p_\ell < 80$ GeV	419	1858	56	183	2096	8.4
$110 < m_{\text{recoil}} < 150$ GeV	430	531	19	186	737	12.6	$110 < m_{\text{recoil}} < 150$ GeV	414	553	54	181	788	11.9
$ \eta_{\text{miss}} < 2$	416	435	19	180	634	12.8	$ \eta_{\text{miss}} < 2$	401	461	53	175	689	12.1
MVA > 0.6	377	12	5	1	18	19.0	MVA > 0.6	359	13	3	1	17	18.5
Cumulative Efficiency (%)	79	0	0	0	0	—	Cumulative Efficiency (%)	72	0	0	0	0	—

and **ZmumuHmumu**; 1.3σ in **ZeeHee** and **ZmumuHemu**; and 1.9σ in **ZeeHemu**. The selection criteria used for $\sqrt{s} = 240$ GeV analysis are applied with the exception of the selection on lepton momentum. We also trained BDT from XGBOOST package, keeping the same network pa-

rameters as outlined in Table VI.

Applying the selection on MVA score greater than 0.6, leads to significance of 4.7σ in **ZmumuHee**; 4.4σ in **ZeeHmumu** and **ZmumuHmumu**; 4.1σ in **ZeeHee**. We note as before that the channels **ZmumuHemu** and **ZeeHemu** show

Table V: Event yields and significance for all channels at $\sqrt{s} = 365$ GeV after applying selection conditions. Here, B_{other} includes processes such as ZH (Background) and $t\bar{t}$.

(a) $Z\mu\mu H\mu\mu$							(b) $ZeeH\mu\mu$						
Selection	S	B_{ZZ}	B_{WW}	B_{other}	B_{tot}	Z	Selection	S	B_{ZZ}	B_{WW}	B_{other}	B_{tot}	Z
Preselection	47	2760	765	3460	6985	0.6	Preselection	75	2760	765	3460	6985	0.9
$80 < m_Z < 100$ GeV	41	1268	51	114	1433	1.1	$80 < m_Z < 100$ GeV	39	1151	14	110	1274	1.1
$110 < m_{\text{recoil}} < 150$ GeV	39	268	47	105	420	1.8	$110 < m_{\text{recoil}} < 150$ GeV	38	230	13	103	346	1.9
$ \eta_{\text{miss}} < 2$	30	43	8	18	68	3.0	$ \eta_{\text{miss}} < 2$	28	41	2	15	58	3.0
MVA > 0.6	23	1	0	0	1	4.7	MVA > 0.6	20	0	0	0	1	4.4
Cumulative Efficiency (%)	49	0	0	0	0	—	Cumulative Efficiency (%)	27	0	0	0	0	—

(c) $Z\mu\mu H\mu\mu$							(d) $ZeeHe$						
Selection	S	B_{ZZ}	B_{WW}	B_{other}	B_{tot}	Z	Selection	S	B_{ZZ}	B_{WW}	B_{other}	B_{tot}	Z
Preselection	45	1289	162	884	2336	0.9	Preselection	78	1394	787	1041	3222	1.3
$80 < m_Z < 100$ GeV	41	1008	38	107	1153	1.2	$80 < m_Z < 100$ GeV	50	1009	150	129	1288	1.4
$110 < m_{\text{recoil}} < 150$ GeV	39	271	36	100	408	1.9	$110 < m_{\text{recoil}} < 150$ GeV	48	282	142	119	543	2.0
$ \eta_{\text{miss}} < 2$	28	41	4	15	60	3.0	$ \eta_{\text{miss}} < 2$	28	50	22	15	87	2.6
MVA > 0.6	21	1	1	0	2	4.4	MVA > 0.6	17	0	0	0	1	4.1
Cumulative Efficiency (%)	47	0	1	0	0	—	Cumulative Efficiency (%)	22	0	0	0	0	—

(e) $Z\mu\mu H\mu\mu$							(f) $ZeeH\mu\mu$						
Selection	S	B_{ZZ}	B_{WW}	B_{other}	B_{tot}	Z	Selection	S	B_{ZZ}	B_{WW}	B_{other}	B_{tot}	Z
Preselection	92	1095	296	3235	4626	1.3	Preselection	150	1149	1327	3516	5991	1.9
$80 < m_Z < 100$ GeV	82	627	27	205	859	2.7	$80 < m_Z < 100$ GeV	89	600	82	207	889	2.8
$110 < m_{\text{recoil}} < 150$ GeV	79	503	25	197	724	2.8	$110 < m_{\text{recoil}} < 150$ GeV	85	485	75	197	756	2.9
$ \eta_{\text{miss}} < 2$	58	76	4	25	105	4.6	$ \eta_{\text{miss}} < 2$	55	86	12	24	123	4.1
MVA > 0.6	49	3	1	0	4	6.7	MVA > 0.6	43	2	0	0	2	6.4
Cumulative Efficiency (%)	53	0	0	0	0	—	Cumulative Efficiency (%)	29	0	0	0	0	—

the highest significance across channels corresponding to 6.7σ and 6.4σ , respectively.

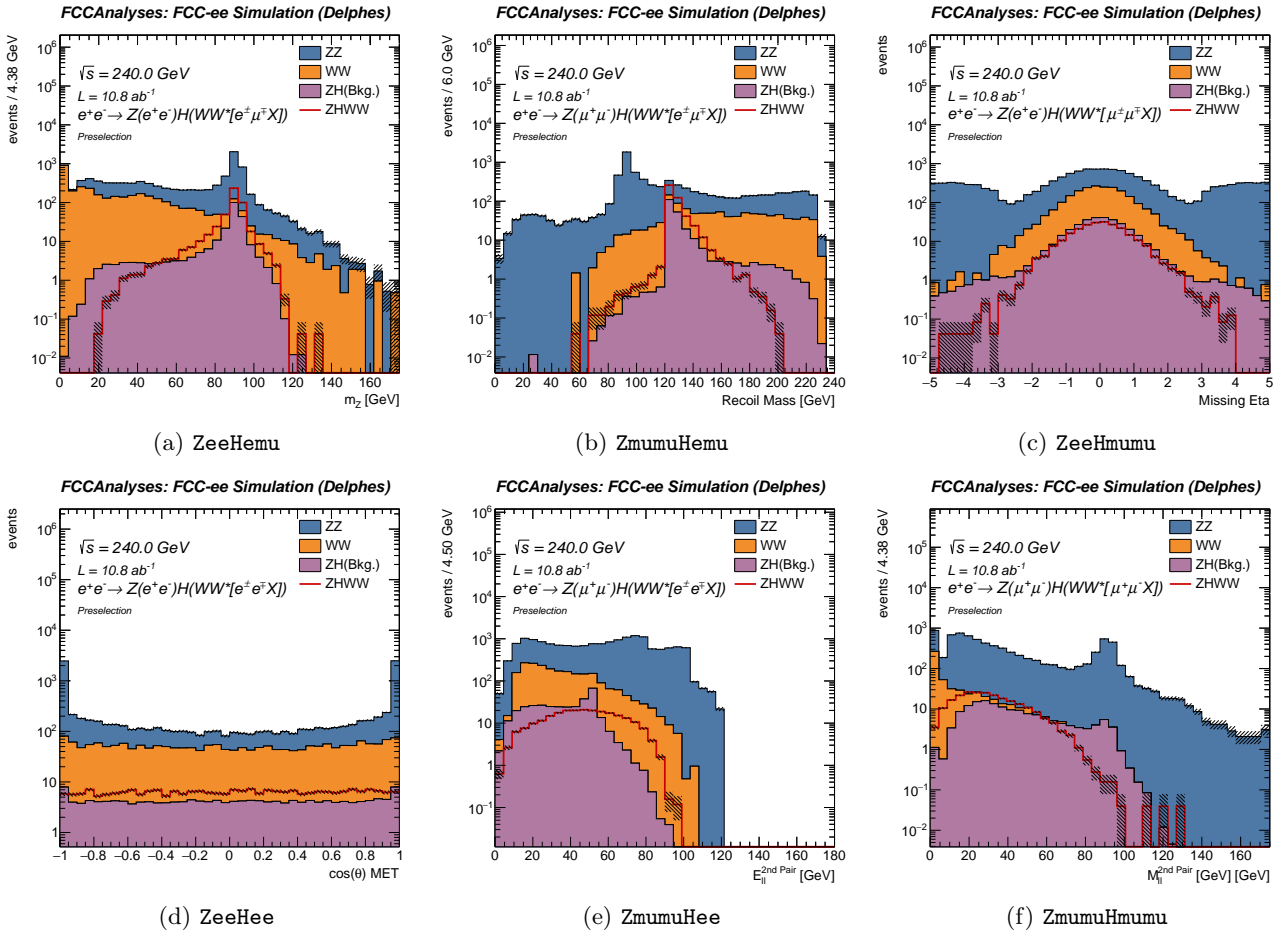


Figure 1: Distributions of observables after applying preselection criteria for $\sqrt{s} = 240$ GeV. (a) Z candidate mass for the ZeeHemu channel. (b) Recoil mass for the ZmumuHemu channel. (c) η_{miss} for the ZeeHmumu channel. (d) $\cos\theta_{\text{MET}}$ in the ZeeHee channel. (e) energy of the second lepton pair in the ZmumuHee channel. (f) invariant mass of the second lepton pair in the ZmumuHmumu channel. The uncertainty associated with the MC simulation is shown by the shaded area.

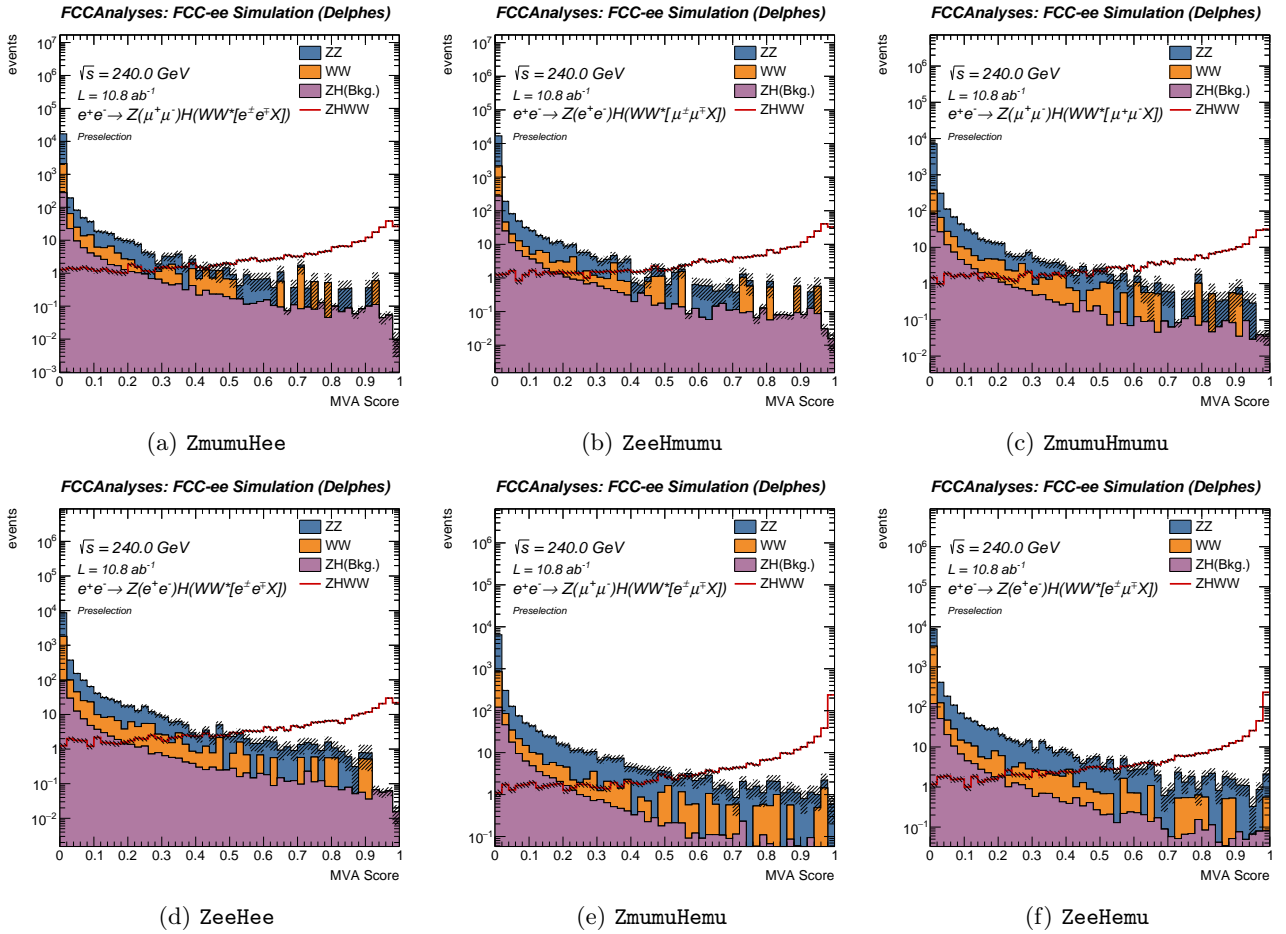


Figure 2: MVA score for the ZmumuHee, ZeeHmumu, ZmumuHmumu, ZeeHee, ZmumuHemu, ZeeHemu channels for $\sqrt{s} = 240$ GeV. The uncertainty associated with the MC simulation is shown by the shaded area.

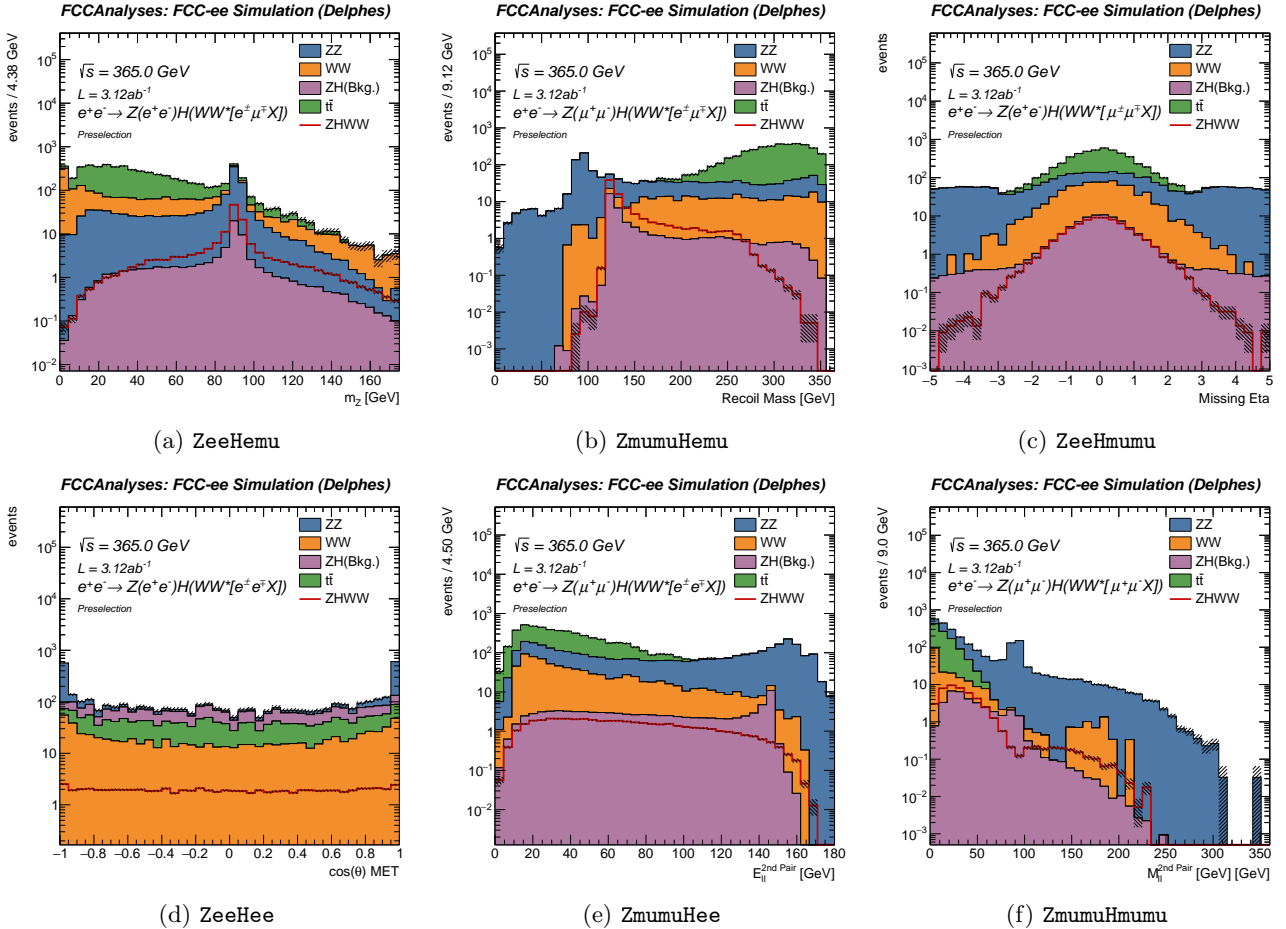


Figure 3: Distributions of observables after applying preselection criteria for $\sqrt{s} = 365$ GeV. (a) Z candidate mass for the ZeeHemu channel. (b) Recoil mass for the ZmumuHemu channel. (c) η_{miss} for the ZeeHmumu channel. (d) $\cos(\theta)$ MET in the ZeeHee channel. (e) energy of the second lepton pair in the ZmumuHee channel. (f) invariant mass of the second lepton pair in the ZmumuHmumu channel. The uncertainty associated with the MC simulation is shown by the shaded area.

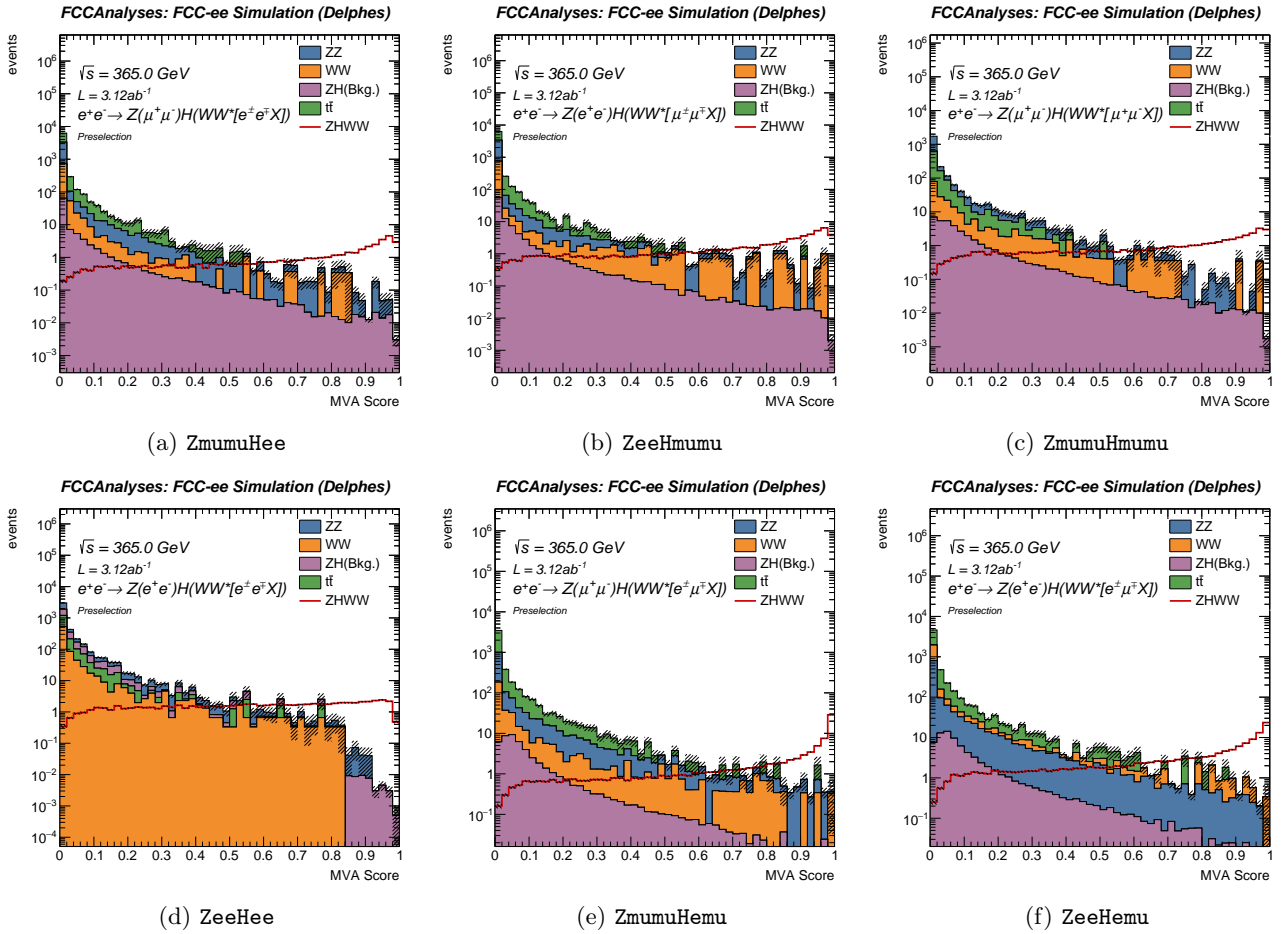


Figure 4: MVA score for the ZmumuHee, ZeeHmumu, ZmumuHmumu, ZeeHee, ZmumuHemu, ZeeHemu channels for $\sqrt{s} = 365$ GeV. The uncertainty associated with the MC simulation is shown by the shaded area.

Table VI: XGBoost hyperparameters used for training the Machine Learning Model for $\sqrt{s} = 240, 365$ GeV.

Parameter	Value	Description
Objective	binary:logistic	Binary classification
Evaluation Metric	logloss	Loss function for evaluation
Max Depth	5	Maximum depth of tree
Learning Rate	0.03	Learning Rate for Model
Number of Estimators	1000	Number of Trees
Subsample	0.6	Fraction of data used per tree
Column Sample by Tree	0.6	Fraction of features used per tree
Gamma	1.0	Minimum loss reduction to split
Min Child Weight	5	Minimum sum of instance weight in child
L1 Regularization (α)	0.5	L1 regularization term
L2 Regularization (λ)	3.0	L2 regularization term
Tree Method	hist	Histogram-based tree
Early Stopping Rounds	50	Stops the code if no improvement after 50 steps

V. DETERMINING THE SIGNAL STRENGTH

The signal strength for $\sigma_{ZH} \times Br(H \rightarrow WW)$ is obtained using the CMS COMBINE package [22]. To measure this, we used the MVA score as the observable after applying all selection criteria, except the final selection on the MVA score. We obtain the pseudo-data by adding the signal and background events obtained after appropriate scaling with luminosity and cross-section. The background processes are assigned a 10% normalisation uncertainty, while luminosity is assigned a 1% uncertainty. The relative uncertainty for each channel is then evaluated. As each of the six channels are orthogonal to one another, we have also evaluated the combined relative uncertainty in the $Z(\ell\ell)H(WW \rightarrow \ell\ell\nu\nu)$. Our results are summarised in Table VII for $\sqrt{s} = 240$ GeV and in Table VIII for $\sqrt{s} = 365$ GeV. For $\sqrt{s} = 240$ GeV the relative uncertainty is lowest in the **ZmumuHemu** channel at a value of 5.1% followed by the **ZeeHemu** channel with an uncertainty at a value of 5.3%. The highest relative uncertainty is found in the **ZeeHee** channel, with a value of 7.2%.

For the $\sqrt{s} = 240$ GeV, the combined relative uncertainty obtained by combining the six channels within CMS COMBINE tool is found to be 2.9% which, approximately, corresponds to a signal significance of 35.1σ , assuming that the uncertainty $\propto 1/\text{significance}$.

Owing to limited sample statistics for the $\sqrt{s} = 365$ GeV, we find that the relative uncertainty is $\sim 14\%$ for all channels. The combined uncertainty is found as 6.8%. This corresponds to a signal significance of 14.7σ .

VI. CONCLUSION

We have studied the prospects of measuring $Z(\ell\ell)H \rightarrow WW(\ell\ell\nu\nu)$ in the four lepton final state at the FCC-ee. The analysis was performed at two centre-of-mass energies, $\sqrt{s} = 240$ GeV and $\sqrt{s} = 365$ GeV, considering an integrated luminosity of 10.8 ab^{-1} and 3.12 ab^{-1} , respectively.

The analysis was carried out in six orthogonal channels

Table VII: Significance and relative uncertainty for the six channels considered in this analysis for $\sqrt{s} = 240$ GeV.

Channel	Relative uncertainty (%)	Significance (σ)
ZmumuHee	6.9	12.8
ZeeHmumu	7.0	12.7
ZmumuHmumu	7.1	12.4
ZeeHee	7.2	11.8
ZmumuHemu	5.1	19.0
ZeeHemu	5.3	18.5
Combined	2.9	~ 35.1

Table VIII: Significance and relative uncertainty for the six channels considered in this analysis for $\sqrt{s} = 365$ GeV.

Channel	Relative uncertainty (%)	Significance (σ)
ZmumuHee	14.5	4.7
ZeeHmumu	14.2	4.4
ZmumuHmumu	14.2	4.4
ZeeHee	14.1	4.1
ZmumuHemu	14.9	6.7
ZeeHemu	14.9	6.4
Combined	6.8	~ 14.7

defined according to the number of electrons and muons in the final states. The use of Multivariate Analysis Techniques by incorporating Boosted Decision Tree enhanced the signal over background significantly.

We obtain a combined relative uncertainty of 2.9% on measuring $\sigma(e^+e^- \rightarrow ZH) \times Br(H \rightarrow W^+W^-)$ at $\sqrt{s} = 240$ GeV. This corresponds to a combined significance of 35.1σ . On the other hand, at $\sqrt{s} = 365$ GeV, the relative uncertainties are worse by a factor of 2-3 times. The corresponding combined relative uncertainty is 6.8%, corresponding to a significance of 14.7σ . The results indicate more precise measurements of $\sigma(e^+e^- \rightarrow ZH) \times Br(H \rightarrow$

W^+W^-) are possible at $\sqrt{s} = 240$ GeV energy compared to when FCC-ee is running at $\sqrt{s} = 365$ GeV energy.

[1] ATLAS Collaboration, Phys. Lett. B **716**, 1 (2012), arXiv:1207.7214 [hep-ex].

[2] CMS Collaboration, Phys. Lett. B **716**, 30 (2012), arXiv:1207.7235 [hep-ex].

[3] F. Englert and R. Brout, Phys. Rev. Lett. **13**, 321 (1964).

[4] P. W. Higgs, Phys. Lett. **12**, 132 (1964).

[5] ATLAS Collaboration, Nature **607**, 52 (2022), arXiv:2207.00092 [hep-ex].

[6] CMS Collaboration, Nature **607**, 60 (2022), arXiv:2207.00043 [hep-ex].

[7] M. Benedikt *et al.* (FCC), Future Circular Collider Feasibility Study Report: Volume 1, Physics, Experiments, Detectors (2025), arXiv:2505.00272 [hep-ex].

[8] M. Benedikt *et al.* (FCC), Future Circular Collider Feasibility Study Report: Volume 3, Civil Engineering, Implementation and Sustainability (2025), arXiv:2505.00273 [physics.acc-ph].

[9] M. Benedikt *et al.* (FCC), Future Circular Collider Feasibility Study Report: Volume 2, Accelerators, Technical Infrastructure and Safety (2025), arXiv:2505.00274 [physics.acc-ph].

[10] S. Navas *et al.* (Particle Data Group), Phys. Rev. D **110**, 030001 (2024).

[11] FCC Collaboration, IDEA—FCC-ee Winter 2023 Monte-Carlo Production, <https://fcc-physics-events.web.cern.ch/fcc-ee/rec/winter2023/IDEA> (2023), accessed December 14, 2025.

[12] W. Kilian, T. Ohl, and J. Reuter, Eur. Phys. J. C **71**, 1742 (2011), arXiv:0708.4233 [hep-ph].

[13] T. Sjostrand, S. Mrenna, and P. Z. Skands, JHEP **05**, 026, arXiv:hep-ph/0603175.

[14] T. Sjöstrand, S. Ask, J. R. Christiansen, R. Corke, N. De-sai, P. Ilten, S. Mrenna, S. Prestel, C. O. Rasmussen, and P. Z. Skands, Comput. Phys. Commun. **191**, 159 (2015), arXiv:1410.3012 [hep-ph].

[15] J. de Favereau, C. Delaere, P. Demin, A. Giammanco, V. Lemaître, A. Mertens, and M. Selvaggi (DELPHES 3), JHEP **02**, 057, arXiv:1307.6346 [hep-ex].

[16] M. Abbrescia *et al.* (IDEA Study Group), The IDEA detector concept for FCC-ee (2025), arXiv:2502.21223 [physics.ins-det].

[17] A. Sailer *et al.* (Key4hep) (2023) arXiv:2312.08151 [hep-ex].

[18] FCC Collaboration, FCC-config: FCC configuration files, <https://github.com/HEP-FCC/FCC-config> (2025), GitHub repository, accessed December 14, 2025.

[19] C. Helsens, E. Perez, M. Selvaggi, V. Volkl, L. Forthomme, and J. Munch Torndal, HEP-FCC/FCCAnalyses: v0.11.0 (2025).

[20] T. Chen and C. Guestrin, in *Proceedings of the 22nd ACM SIGKDD International Conference on Knowledge Discovery and Data Mining* (ACM, 2016) pp. 785–794, arXiv:1603.02754.

[21] R. Brun and F. Rademakers, Nucl. Instrum. Meth. A **389**, 81 (1997).

[22] A. Hayrapetyan *et al.* (CMS), Comput. Softw. Big Sci. **8**, 19 (2024), arXiv:2404.06614 [physics.data-an].